A major purpose of the Technical Information Center is to provide the broadest dissemination possible of information contained in DOE's Research and Development Reports to business, industry, the academic community, and federal, state and local governments.

Although portions of this report are not reproducible, it is being made available in microfiche to facilitate the availability of those parts of the document which are legible.

LA-UR -87-3425

CONF-8711071--30

Los Alamos National Laboratory is operated by the University of California for the United States Department of Energy under contract W-7405-ENG-36.

LA-UR--87-3425

DE88 001834

TITLE: HEAT FLUX ESTIMATES AND ARMOR DESIGN FOR CPRF/ZTH

AUTHOR(S): J. N. Downing, K. A. Werley, and M. T. Gamble

SUBMITTED TO: IEEE 12th Symposium on Fusion Engineering, October 13-16, 1987 - Monterey Conference Center, Monterey, California

DISCLAIMER

Los Alamos Los Alamos National Laboratory
Los Alamos, New Mexico 87545

HEAT FLUX ESTIMATES AND ARMOR DESIGN FOR CPRF/ZTH*

J. N. Downing, K. A. Werley, and M. T. Gamble
P. O. Box 1663, MS-F648, Los Alamos National Laboratory
Los Alamos, New Mexico 87545

Abstract

A model for the scrape-off layer (SOL) in Reversed-Field Pinches (RFPs) was developed to evaluate the wall heat flux distribution in CPRF/ZTH. Design options for high heat flux areas have been evaluated. A finite element model was used to determine the front-surface temperature and the thermally-induced stresses in the graphite.

Introduction

A simplified model for the scrape-off layer (SOL) in Reversed-Field Pinches (RFPs) has been developed and applied to CPRF/ZTH. The objectives of this exercise are (a) to determine the sensitivity of the wall heat flux distribution versus poloidal angle as a function of plasma position, (b) to estimate the heat flux enhancement resulting from the removal of armor or wall material, and (c) to estimate the impact of magnetic field errors on the heat flux distribution. The heat flux distribution in the SOL was assumed to be described by an exponential with a characteristic scrape-off length ($\lambda_\perp$ = 0.02 – 2.0cm). Both radial and parallel (along field-lines) transport was considered. In RFPs, a significant electron drift velocity, compared with the thermal velocity, is observed. This characteristic results in an enhancement in the heat flux by a factor of 2 for small ($\approx 0.25\lambda_\perp$) equilibrium shifts. Additional peaking of the heat flux results from larger ($\geq 0.25\lambda_\perp$) equilibrium shifts and/or the removal of sections of the armor. When a section of the armor is removed (such as in the area of ports) and the equilibrium is shifted, the field lines can intercept nearby armor segments at angles that produce peaking factors (PFs) in the range of 10 – 1000 The armor segments adjacent to the missing armor segment, therefore, must be contoured to reduce the heat flux to an acceptable level. The front-surface temperatures have been estimated for flat tiles with the nominal and maximum time-dependent heat fluxes anticipated for ZTH. The maximum front surface temperature is estimated to be 1500 K at the design point.

Heat Flux Model

The basic assumption of this model is that the energy density distribution in the scrape-off layer (SOL) can be described by the following relationship:

$$w = w_0 \epsilon^{-\frac{(r-a)}{\lambda_\perp}} \qquad (1)$$

where r is the radius of the plasma in the SOL, a is the radius of the last closed field line, $\lambda_\perp$ is the characteristic scrape-off-length, w_0 is the energy density at radius a, and $w(r)$ is the energy density at radius r . The plasma-wall interaction is modeled as shown in Fig. 1, where the plasma is a cylinder of radius (a), which can be offset from a larger cylinder of wall armor of radius ℓ. The horizontal shift of the plasma column is Δa, and θ is the angle measured from the major radial direction (horizontal). This model calculates the normal heat flux to the wall for a given plasma shift of the centroid of the core plasma relative to the centroid of the first wall. Flux surfaces are assumed to be concentric about the core-plasma surface.

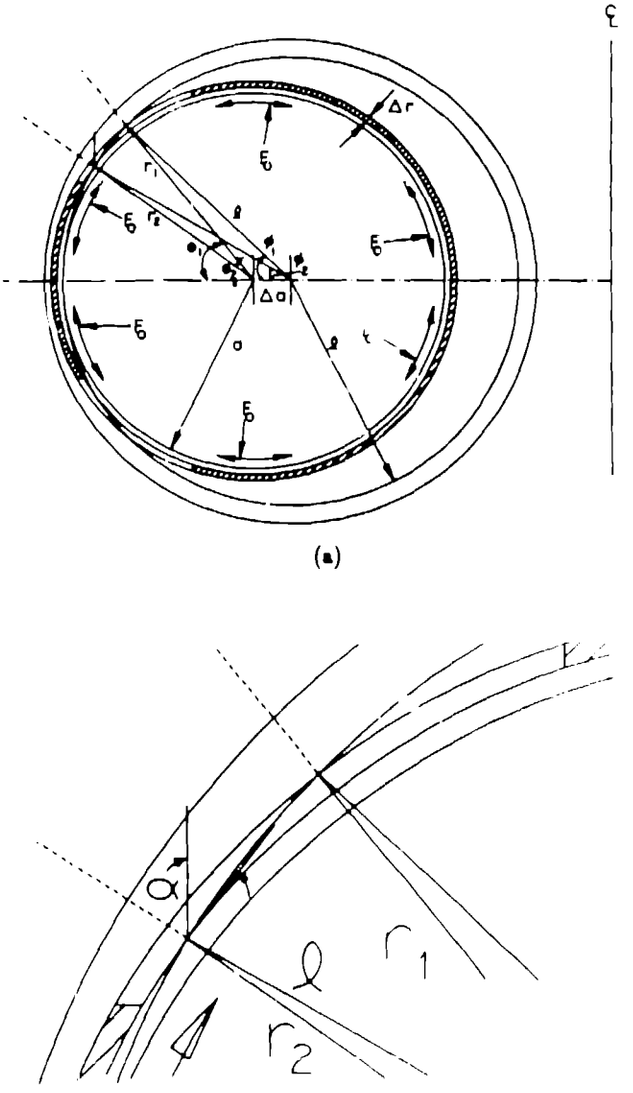

(a)

(b)

Fig. 1 Model used for calculating the plasma-wall interaction. Diagram (b) shows the area of interaction in detail.

Heat flux to the wall is assumed to consist of three parts: (a) parallel-to-magnetic-field-line convection ($q_\parallel$), along flux surfaces which intersect the wall; (b) radial diffusive transport (q_r) characterised by a diffusion coefficient (D) and a radial scale length ($\lambda_\perp$), and (c) a radial radiation heat flux characterised by a core-plasma radiation fraction ($f_{RAD} = P_{RAD}/P_{TOT}$). P_{TOT} is the total source of power to the plasma core, and P_{RAD} is the core radiated power. Edge-plasma radiation is neglected.

The normal heat flux to the first wall is given by

$$q_w = q_\parallel \sin\alpha + q_r \begin{cases} 0, & \alpha \geq \pi/2 \\ \cos\alpha, & \alpha < \pi/2 \end{cases} \qquad (2)$$

* Work performed under the auspices of U.S. Department of Energy

where

$$q_{\parallel} = \omega v_{\parallel} \tag{3}$$

$$q_r = \frac{\omega D}{\lambda_\perp} + \frac{f_{RAD} P_{TOT}}{A} \tag{4}$$

and

$$\lambda_\perp = \sqrt{\frac{DL}{v_{\parallel}}} \tag{5}$$

$$A = 2\pi r Z. \tag{6}$$

Previously undefined variables include: the angle between a field line and the wall (α); the flux surface area (A); the net fluid velocity of electrons parallel to the field lines ($v_{\parallel}$); and the plasma length (Z). The average field line length that energy is transported along (L), is estimated to be $L = 2\pi r/n_D$ for the RFP, where n_D is the number of directions of energy flow and it has a value of either 1 or 2. This $n_D = 1$ option is included because the ZT-40M RFP experiment exhibits preferential energy flow in the direction of electron drift.

The average heat flux to the wall (q_0), is given by

$$q_0 = \frac{P_{TOT}}{A_w} = \frac{1}{A_w(1 - f_{RAD})} \int_a^{+\infty} q_{\parallel} Z n_D dr \tag{7}$$

Thus, PF can be written:

$$PF = \frac{q_w}{q_0} = \frac{2\pi\ell(1 - f_{RAD})}{n_D \lambda_\perp} e^{-\frac{(r-a)}{\lambda_\perp}} \sin\alpha$$

$$+ \left[\frac{\ell}{a}(1 - f_{RAD}) e^{-\frac{(r-a)}{\lambda_\perp}} + \frac{\ell}{r} f_{RAD}\right] \begin{cases} 0, & \alpha \geq \pi/2 \\ \cos\alpha, & \alpha \leq \pi/2 \end{cases} \tag{8}$$

The heat flux distribution, normalised to the average wall heat flux, for a continuous cylindrically shaped wall is shown as a function of poloidal angle (ϕ) in Fig. 2. For these calculations, ($\Delta a/\lambda_\perp$) was varied over the range 0 – 4 and $f_{RAD} = 0$. Maximum PFs and corresponding poloidal angles are plotted, in Fig. 3, versus the shift of the plasma column in units of $\lambda_\perp$. The maximum peaking factors vary from $\approx 1 - 8$ for shifts of $0 - 4\lambda_\perp$, and the angle of maximum flux decreases from 90° (for very small shifts) to less than 30°.

If the plasma shifts vertically, the heat flux distributions are the same as calculated in Fig. 1, but the symmetry axis is no longer horizontal. The new axis is given by a line through the axis of the armor and the new axis of the plasma. The angle is determined from $\tan(\Delta x/\Delta a)$ where Δx is the vertical shift.

When a section of the armor is removed, the field lines intercept the armor at a closer to normal angle. This case is illustrated in Figs. 1a. and 1b., where the section of wall armor removed is between angles θ_1 and θ_2. For the armor immediately below a missing armor segment (in the electron flow direction), the enhancement factor is given by

$$\frac{(2\pi\ell)(\phi_1 - \phi_2)/360}{(r_1 - r_2)/\cos(\theta_2 - \phi_2)} \tag{9}$$

and is approximately equal the poloidal length of the missing armor segment divided by the incremental radius ($r_1 - r_2$)

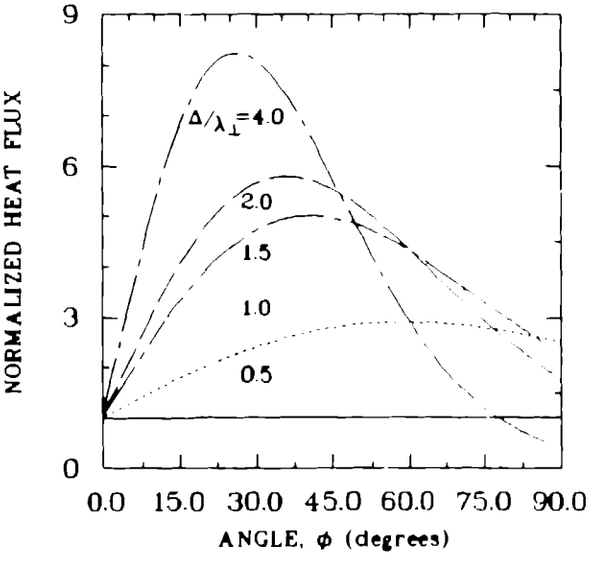

Fig. 2 Heat flux distribution, normalized to the average wall heat flux as a function of poloidal angle.

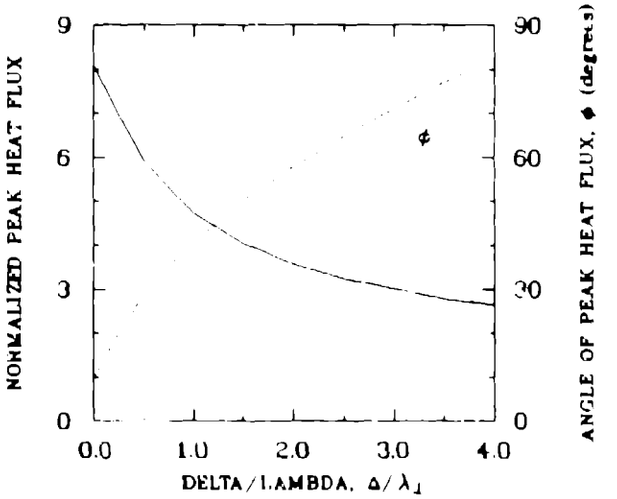

Fig. 3 Maximum PF and corresponding poloidal angle versus the shift of the plasma column in units of $\Delta a/\lambda_\perp$.

defined by the edges of the missing armor. Enhancements in the range of 10 – 1000 occur; therefore, the shape of the tiles surrounding the missing armor must be contoured to keep the heat flux to an acceptable level.

Transport also occurs within the area of the missing armor and the heat flux extends beyond the radius r_1. This transport can be modeled using the same basic assumptions as in Eq. 1:

$$\omega(r_N) = \omega(r_1) e^{-\frac{(r_N - r_1)}{\lambda_\perp^*}} \tag{10}$$

where $\omega(r_N)$ is the flux distribution inside the area of missing armor, $\omega(r_1)$ is the flux calculated from Eq. 1, r_1 is the radius corresponding to the top of the missing armor, r_N is the radius of the plasma inside the area of missing armor, and $\lambda_\perp^*$ is the characteristic scrape-off length corresponding to the smaller dimension of the missing armor. The power flux ($\omega(r_1)$) is the power flux that would have been deposited on the armor that is missing. This effect is large enough that the surfaces must be contoured to keep the heat flux to acceptable levels.

Maximum Heat Flux Specifications

When graphite is used as the armor material, thermal sublimation limits the front-surface temperature, during the flat-top phase of a plasma discharge, to 2300 K. A more conservative value of 1500 K was chosen as a design point to avoid normal operation near this upper limit. Redeposition of the evolved atoms on cooler areas of the graphite armor will act to lower the contamination level and the local maximum temperature can be larger than 1500 K if the surface area affected is only a small fraction of the total area. The initial armor temperature is determined by the liner/armor heating system and will be feedback-controlled to a specific temperature within a range of 23°C to 200°C.

For the purposes of evaluation, four phases of the ZTH discharge are identified. Approximate parameter values for 4 MA operation are given in Table I, and the ZTH design point parameters are given in Table II. The time-averaged (over the duration of the discharge) wall heat flux is 0.8 MW/m^2. With a limit on the graphite front surface temperature of 1500 K and with an initial temperature of 473 K, the maximum time-averaged wall heat flux (for ATJ graphite) is 13 MW/m^2. Therefore, the allowable PF is 16 for these conditions.

TABLE I. APPROXIMATE PARAMETER VALUES FOR ZTH 4MA OPERATION

Discharge Phase	Time Scale (ms)	Average(Maximum) Power Input at Design Point (MW)
Start-up to 2 MA	50	50 (140)
Ramp to 4 MA	400	21 (60)
Flat-top	200	28 (80)
Rampdown	$\leq$ 400	14 (40)

TABLE II. DESIGN POINT PARAMETERS FOR ZTH

Parameter	Value
Plasma Current	4 MA
Poloidal Field Magnetic Energy	36 MJ
Plasma Kinetic Energy	1.1 - 2.2 MJ
First Wall Operating Temperature	300 - 523 K
First Wall Bakeout Temperature	573 K
First Wall Area	36 m^2
Maximum Front Surface Temperature End of Flat-top Phase	1500 K
Minimum Current Termination Time	1.0 ms
Approximate Total Energy to the First-Wall for Full Discharge Duration	22-44 MJ

Heat Flux Peaking Factors

In ohmically heated tokamaks, the flux of particles along the field lines is almost equal in both directions, which suggests a thermal distribution with no unidirectional drift velocity. In RFPs, however, a significant electron drift velocity, compared with the thermal velocity, is observed. This characteristic results in an enhancement in the heat flux by a factor of

TABLE III. HEAT FLUX PEAKING FACTORS (PFs)

Source	Value
Anisotrophy in Heat Flux and Equilibrium Shifts and/or Liner/Coil Tolerances	$\geq$ 4.0
Operational Variations	$\approx$ 2.5
Tile Shape Factor	$\approx$ 2.0
Missing Armor Segments	10 - 1000

$\approx$ 2 for larger ($\Delta a \geq 0.25\ \lambda_\perp$) equilibrium shifts and/or the removal of sections of the armor.

Tolerances in coil construction, coil placement, liner construction, liner support, shell construction, and the application of an incorrect vertical field are examples of field errors that will produce a general equilibrium shift with respect to the armor in ZTH. The technical design criterion for the net effect of these variations is $\pm$ 5.0-mm. The shift in the flux surfaces from these errors can easily be on the order of 1.0 $\lambda_\perp$, which results in a PF $\approx$2.0.

The PF indicated in Fig. 2 is the net PF for both the anisotrophy and the equilibrium shifts and is $\approx$ 4.0 for the conditions indicated above. If the anisotrophy disappeared, the PFs associated with both the anisotrophy and shifts of the plasma column would decrease. The anisotrophy is associated with a large $\nu_\parallel$ and a corresponding short $\lambda_\perp$. As $\lambda_\perp$ gets larger the PF resulting from the shift of the plasma will decrease.

If flat tiles are used, the anisotrophy in heat flux will result in most of the heating being deposited on only one-half of the surface. The resulting PF = 2. Shaping the tiles to have a radius of curvature of l would eliminate this PF. Tapering the surface of the tiles can also significantly lower the PF.

To obtain relevant physics data, the operating conditions will be varied. In general, this variance will result in an increase in the input power and a corresponding PF of $\approx$ 2.5.

The sources of the PFs and their approximate values are summarized in Table III. The minimum PF is given by the product of the first three PFs in Table III and has a value of 10 (if the tiles are shaped) and 20 (if the tiles are not shaped). In the areas of missing armor, the PF will be much larger, and it will be necessary to shape the armor in the area around the missing segments.

Design Options

Average power inputs $<$ 1 MW/m^2 with equilibrium shifts $\leq \lambda_\perp$ can be accommodated in areas in which the armor has been removed by the symmetric contouring shown schematically in Fig. 4. For this approach, the armor tiles around the missing armor are tapered to provide enough surface area to keep the heat flux to an acceptable level. A symmetric arrangement would allow both the poloidal and toroidal currents to be reversed, which is considered an important physics requirement. If the energy flow in the plasma edge becomes more isotropic in ZTH compared with currently operating machines, this surface modification would be adequate for $<$ 2 MW/m^2, depending on the degree of isotrophy.

To accommodate the maximum heat fluxes with the anticipated anisotrophy in heat flux, the flexibility of changing the direction of the currents will probably have to be sacrificed. A nonsymmetric contouring of the tiles will be used, as shown schematically in Fig. 5. The tile(s) above the missing armor

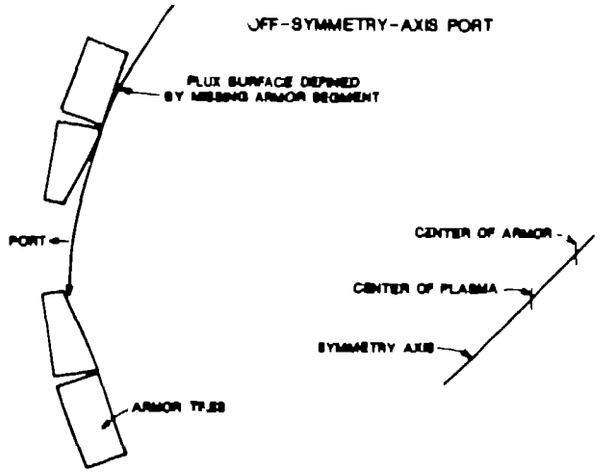

Fig. 4 Schematic drawing of symmetric contouring for off-symmetry-axis port.

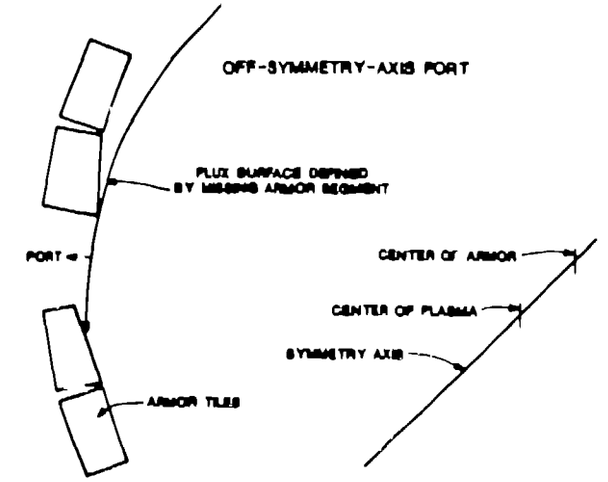

Fig. 5 Schematic drawing of asymmetric contouring for off-symmetry-axis port with the highest heat flux.

is(are) tapered toward the plasma to produce a shadow in the area of the missing armor, and the tile(s) below the missing armor are tapered away from the plasma to provide enough surface area to keep the heat flux to an acceptable level. If the degree of anisotrophy in heat flux is less in ZTH, this last scheme can be modified, as shown schematically in Fig. 6, to accommodate a small fraction of the heat flux in the ion drift direction.

In the present design, the armor has the following characteristics:

1. Rectangular shape with flat surfaces (22 different basic shapes) and 1.2-cm thickness.
2. 128 tiles in the toroidal direction.
3. 44 tiles in the poloidal direction.
4. Single support that supplies the electrical/thermal connection.
5. Deviation from the ideal flux surface of $\leq$ 1.5 mm over the dimensions of the tile.

The tile is mounted to the liner support structure with a metal clip, as shown in Fig. 7. The clip extends $\geq$90% of the toroidal length of the tile and fits in a machined groove on the edge of the tile. Two locking tabs are provided to secure the graphite to the clip.

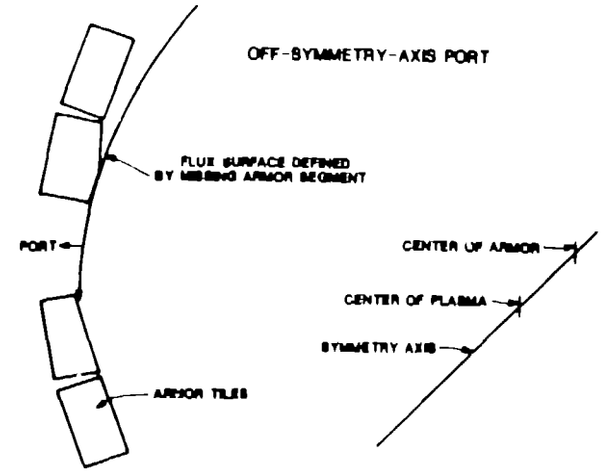

Fig. 6 Figure 5 schematic modified for a small amount of heat flux in the ion-drift direction .

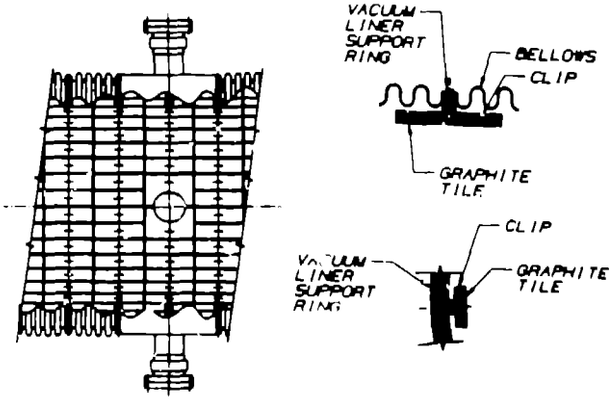

Fig. 7 Schematic drawing of the tile orientation in the liner and the mounting technique.

Each tile is $\approx$ 5.0-cm long in the poloidal direction. The toroidal length depends on the major radius of the tile's location and varies from $\approx$ 13.3 cm on the outside major radius to 9.5 cm on the inside major radius. The gap between tiles is $\approx$ 4 mm. Tolerances in the liner dimensions will be accommodated by custom trimming the dimensions of each tile. Individual tile shapes will be modified as necessary to relieve areas of excessive heat flux. For example, in the area of diagnostic and pumping ports, the tiles will be contoured to keep the heat flux within acceptable limits.

An additional feature of this armor system is the optional incorporation of pumping channels for impurity control. The proposed large-area-pump limiter would remove edge-plasma particles through a uniformly distributed system of slots and channels that perforate the first-wall armor.[1] In addition to the slots formed by the edges of the tiles, small holes through the tile and clip would be uniformly distributed over the tile surface. The size and distribution of the holes would be determined by thermal stress analysis and simulations of plasma exhaust requirements. The volume behind the armor tiles would serve as a "passive" pump during the plasma discharge.

An alternative to individual tiles in the poloidal direction is under consideration. Gore-shaped C-C composite rings are used, as shown in Fig. 8. As seen in the drawing, these rings would probably be attached to the liner support rings in fewer places (3 are shown). Radial forces, such as might occur during current termination, would be absorbed in the armor structure itself. Other advantages of this approach are (a) the present liner design can be used without modification, (b) the poloidal shape will reduce the armor PF compared with the PF for flat tiles, (c) the thickness of the armor and/or the distance between the plasma and the liner might potentially be reduced, and (d) the number of individual elements is reduced. The potential disadvantages of this approach are the following: (a) fewer connections to the liner are used, thereby impairing the removal of heat from the armor structure by conduction. (b) The torus must be disassembled to replace or repair an armor segment. (c) Modifications to the armor to minimize the enhanced heat flux around the ports are difficult. (d) The removal of the armor in the area of the holes will weaken the armor locally.

Thermal Analysis

A finite element model of the armor-clip-liner- insulation-shell system was developed to determine the front-surface temperature and the stresses in the graphite, which result from the heat flux during a high- power discharge. The transient behavior of the system for uniform heat fluxes of 0.2 kW/cm^2 and 2.0 kW/cm^2 is shown in Figs. 9 and 10. The 1.2-cm-thick graphite (ATJ assumed for the calculation) tile achieved a maximum front-surface temperature of 2500°C and a highly non- linear temperature profile through its thickness when exposed to input powers of 2.0 kW/cm^2 for 1-s. This heat flux of 2.0 kW/cm^2 is larger than the anticipated design point heat flux for ZTH. When 0.2 kW/cm^{2}was introduced, the front surface attained a maximum temperature of less than 500°C. The time for cooling to 200°C was also dramatically different for the two cases. Only a small fraction of the total surface area will receive heat fluxes as high as 2.0 kW/cm^2, and these tiles are expected to equilibrate radiatively with the cooler tiles,[2] resulting in an overall thermal decay similar to the 0.2 kW/cm^2 case.

Tensile stresses associated with the high temperatures were in the range of 2000 – 3000 psi. However, the inconel clip must be designed with care. The finite element model assumed a low heat conductance (0.002 BTU/hr-ft^2-F) at the clip and graphite interface that promoted a large temperature differential between the two parts. Greater thermal expansion by the graphite could lead to clip pressure that is not distributed evenly over the graphite-clip interface. If high pressure areas develop, tensile stresses in excess of the allowable maximum (≈6000 psi) could result. A three-dimensional model of this interface would be required to fully quantify these effects.

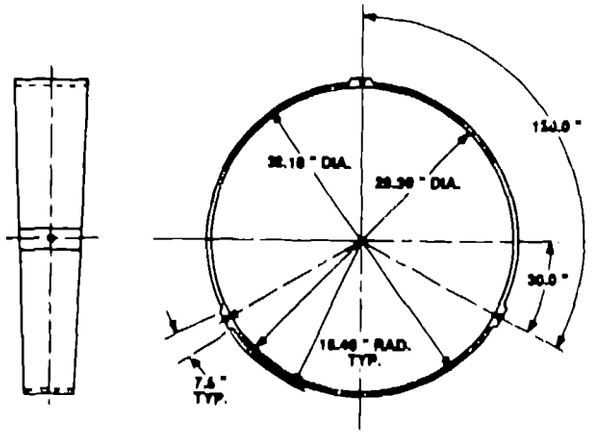

Fig. 8 Schematic drawing of the poloidally continuous C-C composite gore-shaped armor segments.

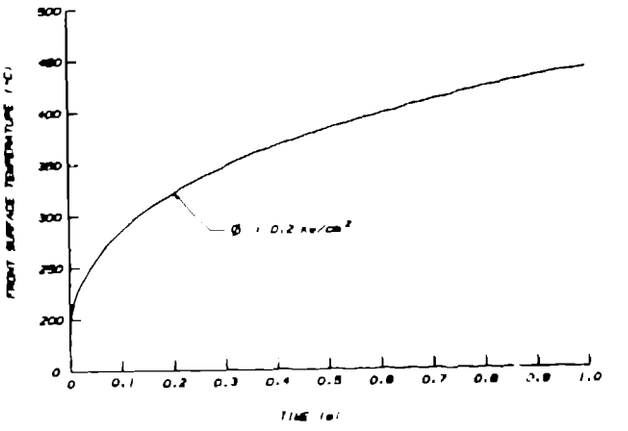

Fig. 9 Graphite front-surface temperature as a function of time for a uniform heat flux (ϕ) of 0.2 kW/cm^2.

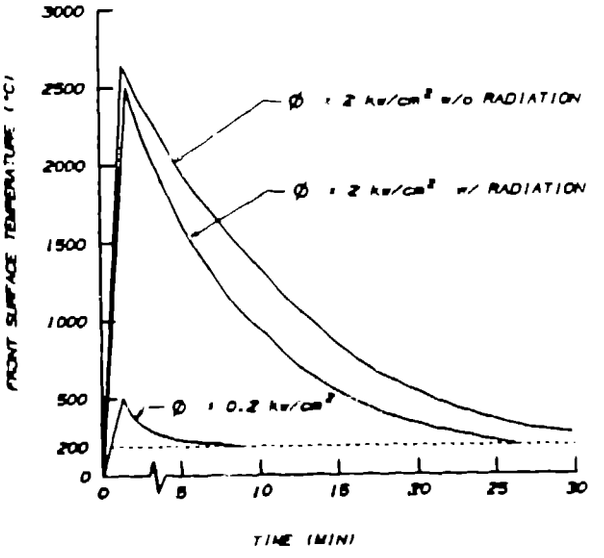

Fig. 10 Transient behavior of armor-clip-liner-insulation-shell system for uniform heat fluxes of 0.2 kW/cm^2 and 2.0 kW/cm^2.

Summary

A simplified model has been used (a) to determine the sensitivity of the poloidal heat flux distribution as a function of plasma position, (b) to estimate the heat flux enhancement resulting from the removal of armor or wall material, and (c) to estimate the impact of magnetic field errors on the heat flux distribution. The armor segments around a missing armor segment must be contoured to keep the heat flux to an acceptable level. The front-surface temperature and the resulting stresses have been obtained for flat tiles with 0.2 kW/cm^2 and 2.0 kW/cm^2 time-dependent heat fluxes.

References

[1] J. N. Downie, Proc. 11th Symp. on Fusion Energy, (1980) 924-927.
[2] F. Elio et al, Proc. 14th Symp. on Fusion Tech., Avignon, (1986).